AGU ADVANCING EARTH AND SPACE SCIENCE

Geophysical Research Letters

RESEARCH LETTER

10.1029/2021GL093550

Key Points:

- Global rates of large earthquakes and explosive volcanic eruptions exhibit decadal timescale trends
- Global seismic moment release is positively correlated with global eruption rate
- Triggering of eruptions following nearby large earthquakes can only explain part of the correlation

Supporting Information:

Supporting Information may be found in the online version of this article.

Correspondence to:

A. P. Jenkins,
alexander.jenkins@bristol.ac.uk

Citation:

Jenkins, A. P., Biggs, J., Rust, A. C., & Rougier, J. C. (2021). Decadal timescale correlations between global earthquake activity and volcanic eruption rates. *Geophysical Research Letters*, *48*, e2021GL093550. https://doi.org/10.1029/2021GL093550

Received 26 MAR 2021
Accepted 18 JUL 2021

Decadal Timescale Correlations Between Global Earthquake Activity and Volcanic Eruption Rates

A. P. Jenkins[1], J. Biggs[1], A. C. Rust[1], and J. C. Rougier[2]

[1]School of Earth Sciences, University of Bristol, Bristol, UK, [2]School of Mathematics, University of Bristol, Bristol, UK

Abstract At the global scale, large tectonic earthquakes and volcanic eruptions are believed to be random and independent events. Here, we compare global time-series of large earthquakes ($M_w \geq 7$) and explosive volcanic eruptions (VEI ≥ 2) spanning 1960–2019. Both time-series exhibit decadal timescale trends, over which annual earthquake and eruption rates vary by a factor of ~2. Moreover, global seismic moment release is positively correlated with global eruption rate, with Monte Carlo permutation tests showing that this correlation is significant with a P-value of <0.05. Although large earthquakes can trigger eruptions at nearby volcanoes, the magnitude of this effect is insufficient to cause the observed global correlation. Other mechanisms, such as triggering of distant eruptions (>1000 km) by earthquake-induced dynamic stress changes, modulation of global earthquake and eruption rates by variations in Earth's rotational velocity, or natural synchronization of events over repeating cycles, are therefore required to explain the correlation.

Plain Language Summary Plate tectonics explains why earthquakes and volcanoes are mainly located near plate boundaries such as subduction zones. However, significantly less is known about what controls the timings of earthquakes and eruptions. We analyze global earthquake and eruption records spanning 1960 through 2019, to investigate whether there is any relationship between when large earthquakes happen and when volcanic eruptions happen. Globally, we find that periods of high earthquake activity tend to coincide with periods of high volcanic activity. It is unlikely that this correlation can be explained by chance. Although we confirm that large earthquakes can trigger eruptions at nearby volcanoes, we show that eruption triggering does not occur often enough to fully explain the observed correlation. This suggests that other factors are responsible for controlling global earthquake and eruption activity, which has implications for understanding seismic and volcanic hazards.

1. Introduction

Earthquakes and volcanoes have long been associated with each other due to their occurrence near plate boundaries. However, whether the timings of large tectonic earthquakes and explosive volcanic eruptions are related is unclear. On one hand, stress changes generated by large earthquakes can trigger eruptions at nearby (≲1000 km) volcanoes within days to several years (Linde & Sacks, 1998; Nishimura, 2017; Sawi & Manga, 2018; Seropian et al., 2021). By contrast, at the global scale, large earthquakes and volcanic eruptions are generally believed to be random and independent events. For example, despite some apparent clustering of large earthquakes globally, such as the occurrence of six $M_w \geq 8.5$ events between 2004 and 2012 (Lay, 2015), most authors agree that aftershock-removed catalogs of large earthquakes are consistent with random Poissonian behavior (Ben-Naim et al., 2013; Daub et al., 2012; Michael, 2011; Parsons & Geist, 2012; Shearer & Stark, 2012). Likewise, De la Cruz-Reyna (1991) showed that global explosive eruptions are well-represented by a Poisson point process, and several other studies assume that global eruptions show Poissonian behavior (e.g., Deligne et al., 2010; Furlan, 2010; Mead & Magill, 2014; Rougier et al., 2016; Rougier, Sparks, Cashman, & Brown, 2018).

In this study, we investigate the relationship between seismicity and volcanism by comparing time-series of large earthquakes ($M_w \geq 7$) and explosive volcanic eruptions (VEI ≥ 2) spanning 1960 through 2019. Our focus is on earthquake and eruptive activity at the global scale, but we also consider regional time-series from subduction zones (Figure 1). To characterize the relationship between the earthquake and eruption time-series, we calculate their cross-correlation. We then use Monte Carlo permutation testing to quantify the significance of the observed correlations. Our results provide evidence for a relationship between global

10.1029/2021GL093550

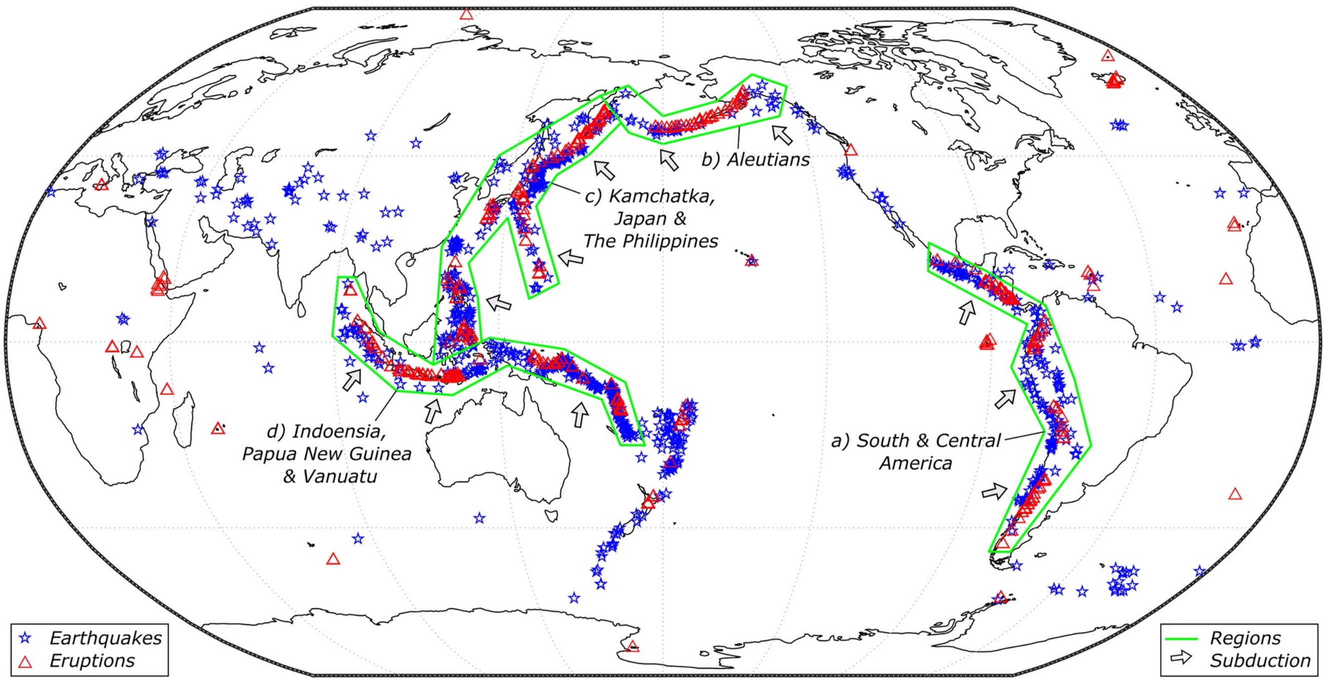

Figure 1. The locations of $M_w \geq 7$ earthquakes (blue stars) and VEI ≥ 2 eruptions (red triangles) during 1960–2019. Green outlines show the boundaries of the four regional time-series (Figure 3).

earthquake and eruption activity, and we discuss how eruption triggering and other physical processes contribute to this.

2. Data and Methods

2.1. Time-Series Generation

Systematic global recording of earthquakes and eruptions began during the 1950s and 1960s. Therefore, we choose a start year of 1960 to avoid including biased or incomplete data from before standard practises were adopted (Figure S1). To generate the global earthquake and eruption time-series, we divide global earthquake and eruption datasets into bins by calendar year, and then sum the events within each bin. For the regional time-series, only events located within the regions defined in Figure 1 are included.

We use earthquake times, locations, and moment magnitudes (M_w) from the International Seismological Center main catalog for 1960 through 1975 (ISC: International Seismological Centre, 2020) and from the Global Centroid Moment Tensor catalog for 1976 through 2019 (CMT: Dziewonski et al., 1981). The ISC catalog is calculated to be complete above approximately M_w 6 since 1960 (Di Giacomo et al., 2018; Storchak et al., 2013, 2015), while the CMT catalog is reported complete above M_w 5.5 (Dziewonski et al., 1981; Ekström et al., 2012). Both catalogs are available for 1976 through 2016 and show good agreement (Figure S2). To account for earthquake magnitudes, we present the earthquake time-series in terms of seismic moment release per year, following the common practice of treating scalar seismic moments from individual earthquakes ($M_o = 10^{1.5M_w + 9.09}$) as extensive [i.e., having the property of physical additivity (Cox & Donnelly, 2011, Section 4.3)]. Results using number of earthquakes per year instead are given in Figure S6. For the global earthquake time-series, we include only $M_w \geq 7$ earthquakes, as smaller earthquakes do not greatly contribute toward global seismic moment release. For the regional time-series, we include $M_w \geq 6$ earthquakes, as some regions have years without any $M_w \geq 7$ events.

We obtain eruption start dates, locations, and explosivity (VEI) from the Global Volcanism Program (GVP: Global Volcanism Program, 2013). There is no visually obvious under-recording of explosive eruptions (VEI ≥ 2) with age, so we assume the record is complete since 1960 (e.g., Mead & Magill, 2014; Newhall &

10.1029/2021GL093550

Self, 1982; Papale, 2018), although Rougier, Sparks, and Cashman (2018) suggest that recording rates decrease prior to 1980. As the VEI scale is only semi-quantitative (Newhall & Self, 1982), we do not account for eruption magnitudes, and instead present the eruption time-series in terms of the number of VEI ≥ 2 eruptions per year. The GVP lists the initiation of 1,157 eruptions with VEI ≥ 2 from 1960 through 2019, including 87 eruptions with an uncertain start year and 64 cases of multiple eruptions from a single volcano within the same calendar year. Including or excluding these multiple and uncertain eruptions in the time-series does not greatly affect the results (Figure S3). The GVP also notes where eruption magnitude is uncertain, but we take the VEI values as given.

2.2. Cross-Correlation Analysis

To characterize the relationship between the earthquake and eruption times-series, we calculate their cross-correlation. The cross-correlation gives the correlation coefficient (ρ) between the earthquake time-series (E) and the eruption time-series (V) as a function of the timeshift (i, in years) applied to the eruption time-series

$$\rho_i = \rho(E, L^i V), \tag{1}$$

where L is the lag operator, which for a time-series $x = (x_1, \ldots, x_T)$ has the property

$$(L^i x)_j = \begin{cases} x_{j-i} & 1 \leq j - i \leq T \\ \boldsymbol{NA} & \text{otherwise,} \end{cases} \tag{2}$$

where $\boldsymbol{NA}$ denotes "not available." In other words, correlations at negative timeshifts ($i < 0$) correspond to changes in earthquake activity preceding changes in eruption activity, while correlations at positive timeshifts ($i > 0$) signify changes in eruption activity preceding changes in earthquake activity. The correlation coefficient we compute is the Spearman's rank correlation coefficient, which quantifies the strength of the monotonic relationship between seismic moment release and eruption rate, with a value of 1 for a perfect positive correlation and −1 for a perfect negative correlation. The more common Pearson's correlation coefficient only assesses linear relationships, but we have no reason to believe that the relationship between seismic moment release and eruption rate will be linear.

To determine the significance of the observed correlations, we define a null model in which there is no relationship between the timings of earthquakes and eruptions. The null model maintains the locations and magnitudes of the observed earthquakes and eruptions, with only their dates being changed. We apply two different methods to reassign event dates. In the first method (RAND), the earthquake and eruption dates are randomly generated within the time-series boundaries, simulating Poissonian behavior. For the second method, we use a permutation test (PERM), in which the observed earthquake and eruption dates are first pooled together, and then randomly reassigned back to the events. Unlike RAND, PERM accounts for the clustering of dates in the observed dataset, although the clustering in the individual time-series is not perfectly maintained as some earthquake dates become eruption dates and vice versa. The presence of clustering in PERM induces some degree of positive correlation on average at small timeshifts, which tends to decrease the significance of the observed correlations.

We use Monte Carlo simulation to calculate P-values for the observed correlations under the null model, for both the RAND and PERM methods. If ρ_i^{obs} is the observed correlation coefficient at timeshift i, $\rho_i^{(r)}$ is the r^{th} simulated correlation coefficient using RAND or PERM at timeshift i, and there are R simulations altogether, then

$$p_i = \frac{1 + \sum_{r=1}^{R} 1(\rho_i^{(r)} \geq \rho_i^{\text{obs}})}{1 + R} \tag{3}$$

is a P-value (Davison, 2003, Section 7.3). p_i gives the probability of obtaining the observed correlation, or stronger, under the null model. For visualisation, our results plot ρ_i^{obs} over the percentiles of $\rho_i^{(1)}, \ldots, \rho_i^{(R)}$, which allows for approximation of the P-values according to the percentiles. Conventionally, a P-value of <0.05 (approximately the 95^{th} percentile) is considered to be a statistically significant result. However, as p_i is calculated for each timeshift, with a long enough sequence of timeshifts, some correlations will be signif-

10.1029/2021GL093550

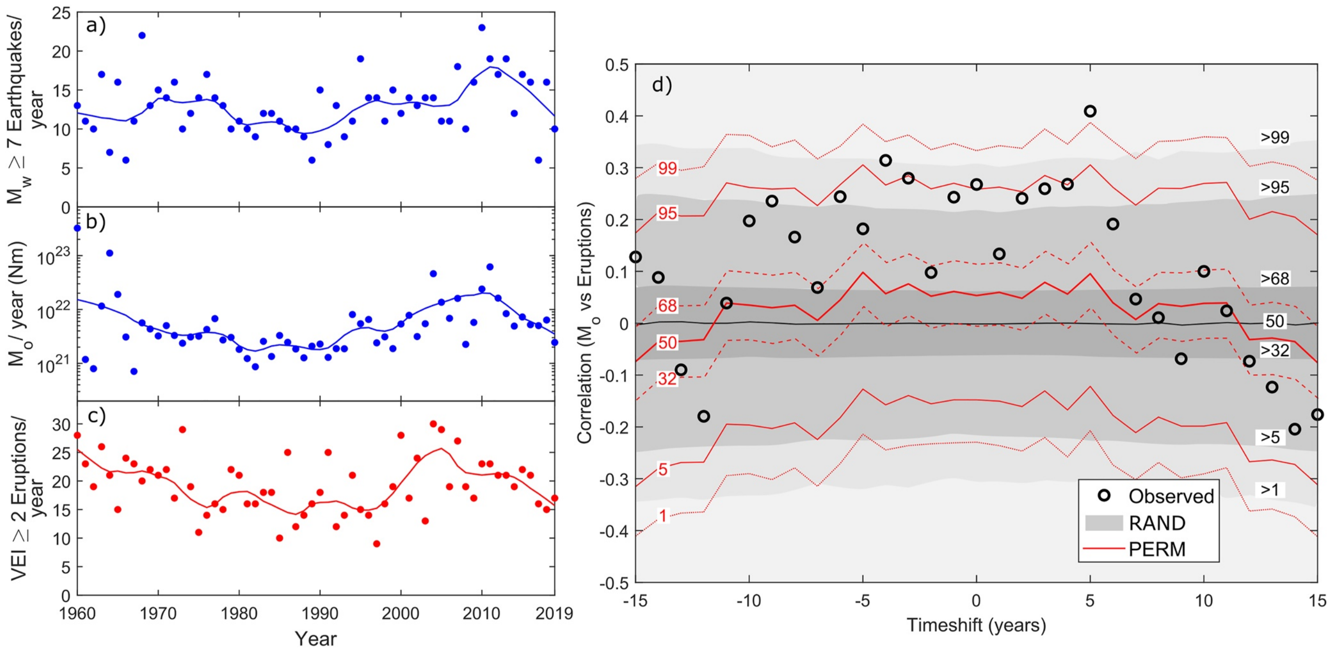

Figure 2. (a–c) Global earthquake and eruption time-series 1960–2019 (circles), with 15% span parameter LOESS curves (lines) for visualisation. The eruption time-series includes multiple and uncertain eruptions. (d) Cross-correlation between global seismic moment release time-series (b) and VEI ≥ 2 eruption time-series (c), with reference to the percentiles of the RAND (shading, black line, and black numbers) and PERM (red lines and numbers) null models. Negative timeshifts correspond to changes in earthquake activity preceding changes in eruption activity, and vice versa for positive timeshifts.

icant purely by chance under the null model. Therefore, we must be careful not to over-interpret any one significant P-value over the whole sequence of applied timeshifts.

3. Results

3.1. Global Time-Series

Figure 2b shows the global seismic moment release time-series, while Figure 2c shows the global eruption time-series, including multiple and uncertain eruptions. As the time-series themselves show considerable variability from year-to-year, we fit locally weighted polynomial regressions (LOESS) to help visualize multi-year trends in earthquake and eruption activity. From the LOESS curves, there is visually a correlation between seismic moment release and eruption rate, which is apparent over decadal timescales. In particular, periods of high seismic moment release and volcanic activity occurred during the 1960s and early 1970s, and then again from around 2000 until the early 2010s. By contrast, the 1980s and 1990s were characterized by relatively lower seismic and volcanic activity, and data since around 2015 suggest a trend toward another period of lower levels of global activity.

Figure 2d shows the cross-correlation between the (unsmoothed) global seismic moment release time-series and the (unsmoothed) global eruption time-series. The observed positive correlations at timeshifts between −11 and +8 years support the visual correlation evident from the LOESS curves, with peak correlation coefficients of 0.3–0.4 indicating a weak to moderate correlation between global seismic moment release and global eruption rate. Furthermore, the observed negative correlations at timeshifts longer than about ±10 years highlight the decadal timescale over which the correlation acts. Although the most positive correlation coefficient of 0.41 occurs at a timeshift of +5 years, overall there are more positive correlations at negative timeshifts than at positive timeshifts. This may suggest that changes in earthquake activity occur a few years before corresponding changes in eruption rate. However, this is poorly constrained, as the highest correlation coefficients occur at timeshifts ranging between −4 and +5 years.

Under the null model, the observed global correlations are significant at $P < 0.05$ for timeshifts of −4, 0, 4, and 5 years using PERM, with additional significant correlations at timeshifts of −9, −6, −3, −1, 2, and

3 years using RAND (Figure 2d). From the Monte Carlo simulations, the probability of obtaining four or more timeshifts with significant correlations under PERM is 3%, while the chance of obtaining ten or more significant timeshifts under RAND is <0.01% (Table S1). We therefore consider it unlikely that the observed global correlation occurs by chance. Similar results are achieved if uncertain and multiple eruptions are excluded from the time-series, although the timeshifts which have significant correlations vary slightly (Figure S3). Shifting the boundary date for the yearly binning also does not greatly affect the results (Figure S7). More interestingly, using a 3-year bin duration for the time-series increases the peak observed correlation coefficients to 0.5 to 0.6, as well as further increasing their significance (Figure S8). This is because employing longer bin durations removes some of the annual variability in earthquake and eruption rates, instead giving more weight to the decadal timescale trends. Finally, we note that the global correlation depends more strongly upon the largest magnitude earthquakes, as shown by the lack of significant correlations under PERM if number of $M_w \geq 7$ earthquakes is used to measure earthquake activity instead of seismic moment release (Figure S6).

3.2. Regional Time-Series

The majority of $M_w \geq 7$ earthquakes (66%) and VEI ≥ 2 eruptions (85%) are located along the subduction zones bordering the Pacific Ocean (Figure 1). Therefore, we generate four sets of regional time-series based on these plate boundaries (Figure 3). These regions are: (a) eastward-directed subduction of the Nazca and Cocos plates below South and Central America; (b) northward-directed subduction of the Pacific plate below the Aleutian arc; (c) westward-directed subduction of the Pacific and Philippine Sea plates below the Kamchatka Peninsula, Japan, and the Philippines, and; (d) northward-directed subduction of the Australian plate below Indonesia, Papua New Guinea, and Vanuatu. Of these, only the South and Central America region has easily defined, non-overlapping boundaries.

Only the South and Central America region displays an obvious visual correlation, which is supported by positive correlations at timeshifts from −1 to +8 years, although these are not significant at $P < 0.05$ under PERM (Figure 3a). Indonesia, Papua New Guinea, and Vanuatu also shows mostly positive correlations at short timeshifts, which likewise do not reach the $P < 0.05$ threshold for PERM (Figure 3d). By contrast, the Aleutian arc has very little overall correlation (Figure 3b), while Kamchatka, Japan, and the Philippines displays negative correlations at short timeshifts and significant positive correlations at longer timeshifts (Figure 3c). However, we are cautious of over-interpreting these significant positive correlations for Kamchatka, Japan, and the Philippines due to the much lower correlations at the intervening timeshifts and the absence of significant correlations when using a 3-year bin size (Figure S9). Despite the generally low correlations for the regional time-series, the four $M_w > 9$ mega-earthquakes, which dominate the global earthquake time-series, are all associated with periods of high or increasing volcanic activity in their respective regional time-series (1960 Chile earthquake (Figure 3a); 1964 Alaska earthquake (Figure 3b); and 2004 Sumatra earthquake (Figure 3d); 2011 Tohoku earthquake (Figure 3c)). The lack of regional correlations may therefore reflect the lack of large earthquakes in the regional time-series.

4. Discussion

4.1. Implications

The correlation we observe between global seismic moment release and global eruption rate suggests that earthquake and eruption occurrences are not independent at the global scale. This is because Monte Carlo simulation shows that the probability of the correlation occurring by chance is low if earthquakes and eruptions are random and independent events. While our findings contrast with many previous studies (e.g., De la Cruz-Reyna, 1991; Michael, 2011), some more recent work does support the view that earthquake and eruptive activity is time-dependent. For example, several authors have reexamined the historic earthquake record and concluded that Poissonian behavior cannot explain the temporal distribution of large earthquakes (Bendick & Bilham, 2017; Luginbuhl et al., 2018; Rogerson, 2018; Zaliapin & Kreemer, 2017). Likewise, Gusev (2008, 2014) presented evidence for statistically significant clustering of global eruptions since 1900. To investigate whether our results support non-random time-dependent behavior in earthquakes, eruptions, or both, we now explore causal mechanisms that could explain the observed correlation. As

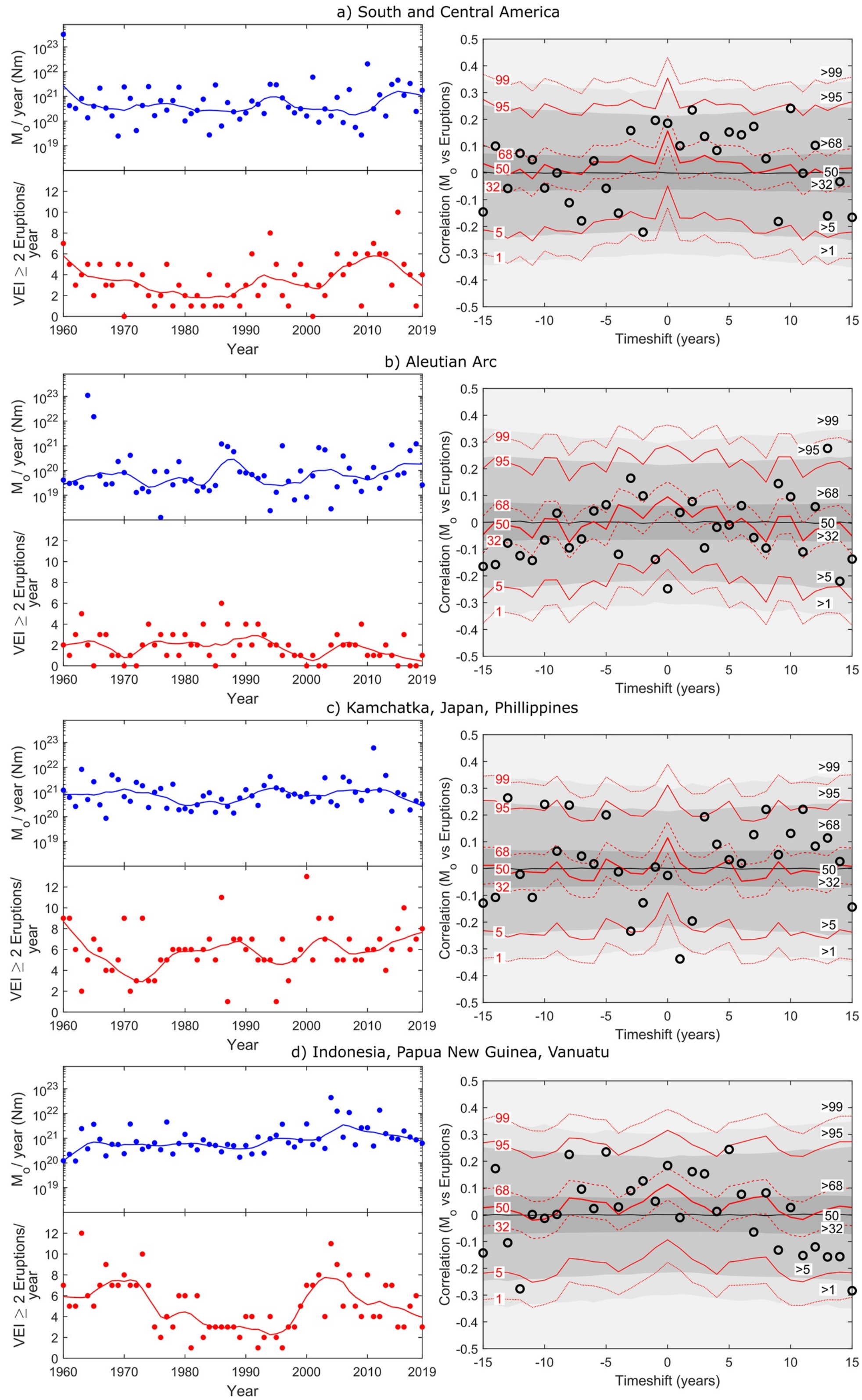

Figure 3. Regional earthquake and eruption time-series and cross-correlation. The time-series include $M_w \geq 6$ earthquakes, and multiple and uncertain eruptions. Color scheme and symbols as in Figure 2 (a) South and Central America; (b) Aleutian arc; (c) Kamchatka, Japan, and The Philippines; (d) Indonesia, Papua New Guinea, and Vanuatu. See Figure 1 for region location maps.

eruption triggering by earthquakes is the most obvious explanation, and is supported by the slight preference for positive correlations at negative timeshifts, we consider this mechanism first.

4.2. Eruption Triggering

Earthquakes themselves display clustering at a local scale because earthquake-induced stress transfer causes aftershocks and earthquake sequences. However, evidence for earthquakes triggering other large earthquakes at distances much beyond 1,000 km is limited, as stress changes decay with distance (Bufe & Perkins, 2005; Johnson et al., 2015; Parsons & Velasco, 2011; Parsons et al., 2014; Wyss & Toya, 2000). Similarly, studies of earthquakes triggering volcanic eruptions focus on distances of 1,000 km or less. For example, Linde and Sacks (1998) found that VEI ≥ 2 eruptions occur four times more often than expected by chance within 5 days and 800 km of magnitude 8 or larger earthquakes, while Nishimura (2017) found a 50% increase in VEI ≥ 2 eruptions within 5 years and 200 km following $M_w \geq 7.5$ earthquakes. By contrast, Sawi and Manga (2018) found no significant increase in VEI ≥ 2 eruption rate within 5 days and 800 km of magnitude 6 or greater earthquakes, although they did find a 5%–12% increase in eruptions in the following 2–24 months.

As eruption triggering is a relatively local scale phenomenon, the lower correlation between seismic moment release and eruption rate at the regional scale compared with the global scale argues against eruption triggering as the causal mechanism. However, the lower regional correlations may simply reflect the lower numbers of larger earthquakes in the regional time-series. Therefore, to investigate whether eruption triggering can explain the global correlation, we quantify the rate of eruption triggering by comparing the number of eruptions that occured after nearby large earthquakes with the number of eruptions that occured in the same time period before those earthquakes. Using the same datasets as for our correlation analysis, we find an increase of up to 10% in VEI ≥ 2 eruption rate within 1,000 km and 1–5 years after $M_w \geq 7$ earthquakes. This corresponds to each $M_w \geq 7$ earthquake triggering, on average, around an extra 0.01 to 0.1 eruptions within a few years and 1,000 km (Table 1). We do not find strong evidence for eruption triggering if $M_w \geq 6$ earthquakes are included, or for smaller or larger distances between the earthquakes and the eruptions. Given that Figure 2a shows that the global rate of $M_w \geq 7$ earthquakes varies by around 20 earthquakes annually, the expected difference in global eruption rate due to triggering is at most around two eruptions per year. As this number is only a very small fraction of the actual annual variability in global eruption rate (Figure 2c), the global correlation likely cannot be explained by eruption triggering alone.

4.3. Alternative Explanations

Various other physical processes have also been proposed to affect earthquake and eruption rates. However, for these to explain the global correlation, they would have to affect both earthquake and eruption rates in the same manner and with similar response times. For example, tidal stresses have been shown to influence earthquake rates and magmatic systems, although their twice-daily to fortnightly periodicities are too short for our time-series (Cochran et al., 2004; Girona et al., 2018; Métivier et al., 2009; Scholz et al., 2019). Climate change at both seasonal and long-term (i.e., glacial cycles) scales can affect earthquake and eruption rates by causing ice sheet unloading or groundwater changes (Bettinelli et al., 2008; Huybers & Langmuir, 2009; Jull & McKenzie, 1996; Kutterolf et al., 2013; Larsen, 2000; Mason et al., 2004; Olivieri & Spada, 2015; Rawson et al., 2016). However, only a few authors have proposed that climate change over decadal timescales may also alter event rates (Pagli & Sigmundsson, 2008; Rampino et al., 1979). Furthermore, the observed periodicity in earthquake and eruption activity is difficult to explain with the ever-increasing temperatures due to anthropogenic climate change. More promisingly, periods of deceleration of the Earth's rotational velocity have been linked with increased rates of both earthquakes (Anderson, 1974; Bendick & Bilham, 2017; Shanker et al., 2001) and eruptions (Levin et al., 2019; Palladino & Sottili, 2014; Tuel et al., 2017). However, the feedback and interactions between earthquakes and eruptions and the solid Earth, atmospheric, and astronomic processes that control the rotation of the Earth are far from clear.

Although our analysis shows that triggering of eruptions by nearby earthquakes occurs too infrequently to explain the global correlation, related mechanisms may play a role. For example, there is emerging evidence that seismic waves produced by large earthquakes can trigger aftershocks, and potentially other large

Table 1
Eruption Triggering Calculated by Comparing the Number of Eruptions That Occured Before and After Earthquakes With $M_w \geq$ Min M_w, Within the Specified Distance and Time Period

Triggering parameters				Results				
Min M_w	Aftershock filter[a]	Distance (km)	Time (years)	Number of Equations[b]	Eruptions before[c]	Eruptions after[c]	% change[d]	Triggered per Equation[e]
6	No	1,000	1	7,543	5,232	5188	−0.8	−0.01
6	Yes	1,000	1	1,397	499	527	5.6	0.02
6	No	1,000	5	7,025	24,520	24,058	−1.9	−0.07
6	Yes	1,000	5	383	486	495	1.9	0.02
7	No	1,000	1	768	507	552	8.9	0.06
7	Yes	1,000	1	445	261	287	10.0	0.06
7	No	1,000	5	713	2,489	2,527	1.5	0.05
7	Yes	1,000	5	174	434	451	3.9	0.10
7	No	200	1	768	55	59	7.3	0.01
7	No	2,000	1	768	1,284	1,301	1.3	0.02
7	No	200	5	713	318	328	3.1	0.01
7	No	2,000	5	713	6,187	6,078	−1.7	−0.02
8	No	1,000	1	48	35	45	28.6	0.21
8	Yes	1,000	1	42	27	31	14.8	0.10
8	No	1,000	5	45	168	174	3.6	0.13
8	Yes	1,000	5	34	121	123	1.7	0.06

[a]Exclusion of earthquakes within the specified distance and time period of a larger earthquake. [b]Earthquakes occurring within "Time" years of the end of the time-series are excluded. [c]Includes multiple and uncertain eruptions, see Table S2 for excluding these eruptions. Note that a single eruption may be counted for multiple earthquakes. [d]Percentage change in number of eruptions from before to after the earthquakes. [e]The mean number of eruptions triggered per earthquake, calculated by (Eruptions after–Eruptions before)/number of Equations.

earthquakes, at global distances (Parsons et al., 2014; Pollitz et al., 2012). Fluid-rich areas, such as magmatic-hydrothermal systems, are particularly susceptible to such dynamic stress changes (Hill et al., 2002). This suggests that eruption triggering at great distances is a possibility, although identifying such triggering is difficult due to the vast numbers of earthquakes and eruptions involved at large scales. While dynamic stress changes at great distances are likely to be low magnitude, over repeated earthquake cycles, this process could lead to a natural synchronization of global earthquake and eruption events (Bendick & Bilham, 2017; Romanowicz, 1993). Furthermore, viscoelastic relaxation following large earthquakes could modulate these cycles of activity over decadal timescales (Marzocchi, 2002; Zaliapin & Kreemer, 2017). These mechanisms appeal because only the very largest earthquakes would produce significant effects at large time and length scales, consistent with the dependence of the observed correlation on the largest magnitude earthquakes.

5. Conclusions

Annual global earthquake and eruption rates have varied by a factor of around two over decadal timescales since 1960. Moreover, global seismic moment release is positively correlated with global eruption rate, with Monte Carlo permutation tests showing that this correlation is significant at $P < 0.05$ for timeshifts up to ± 5 years. Understanding the potential causes of this correlation is important for seismic and volcanic hazard assessment. We find that eruption triggering by nearby large earthquakes occurs too infrequently to fully explain the correlation in the global data, which suggests that other mechanisms, such as triggering of distant eruptions by earthquake-induced dynamic stress changes, modulation of global earthquake and eruption rates by variations in the Earth's rotational velocity, or natural synchronization of events over many repeated cycles, are responsible.

While we demonstrate that the observed correlation is robust since 1960, our analysis of decadal timescale processes is inherently limited by the relatively short length of the available earthquake and eruption time-series (Figure S1). For some regions (e.g., Japan), it might be possible to extend the time-series backwards beyond 1960, although our results suggest that the correlation is reduced at the regional scale. Therefore, further global earthquake and eruption data acquired over the coming decades remains the most promising way to shed more light on the relationship between earthquakes and eruptions, as well as the cause of any potential correlation.

Data Availability Statement

The data used in this study are freely available from the following sources: International Seismological Centre Instrumental Earthquake Catalog (International Seismological Centre, 2020, http://www.isc.ac.uk/iscgem/), Global Centroid Moment Tensor Project (Dziewonski et al., 1981, https://www.globalcmt.org/), Global Volcanism Program (Global Volcanism Program, 2013, https://volcano.si.edu/).

Acknowledgments

This work was supported by the Natural Environment Research Council (NE/L002434/1). A. P. Jenkins and J. Biggs are supported by the NERC Centre for the Observation and Modelling of Earthquakes, Volcanoes and Tectonics (COMET, http://comet.nerc.ac.uk), a partnership between UK Universities and the British Geological Survey. The authors are grateful for the constructive and helpful comments of two anonymous reviewers.

References

Anderson, D. (1974). Earthquakes and the rotation of the earth. *Science*, *186*(4158), 49–50. https://doi.org/10.1126/science.186.4158.49

Bendick, R., & Bilham, R. (2017). Do weak global stresses synchronize earthquakes? *Geophysical Research Letters*, *44*(16), 8320–8327. https://doi.org/10.1002/2017GL074934

Ben-Naim, E., Daub, E., & Johnson, P. (2013). Recurrence statistics of great earthquakes. *Geophysical Research Letters*, *40*(12), 3021–3025. https://doi.org/10.1002/grl.50605

Bettinelli, P., Avouac, J.-P., Flouzat, M., Bollinger, L., Ramillien, G., Rajaure, S., & Sapkota, S. (2008). Seasonal variations of seismicity and geodetic strain in the Himalaya induced by surface hydrology. *Earth and Planetary Science Letters*, *266*(3–4), 332–344. https://doi.org/10.1016/j.epsl.2007.11.021

Bufe, C., & Perkins, D. (2005). Evidence for a global seismic-moment release sequence. *Bulletin of the Seismological Society of America*, *95*(3), 833–843. https://doi.org/10.1785/0120040110

Cochran, E., Vidale, J., & Tanaka, S. (2004). Earth tides can trigger shallow thrust fault earthquakes. *Science*, *306*(5699), 1164–1166. https://doi.org/10.1126/science.1103961

Cox, D., & Donnelly, C. (2011). *Principles of applied statistics*. Cambridge University Press. https://doi.org/10.1017/CBO9781139005036

Daub, E., Ben-Naim, E., Guyer, R., & Johnson, P. (2012). Are megaquakes clustered? *Geophysical Research Letters*, *39*(6), L06308. https://doi.org/10.1029/2012GL051465

Davison, A. (2003). *Statistical models*. Cambridge University Press. https://doi.org/10.1017/CBO9780511815850

De la Cruz-Reyna, S. (1991). Poisson-distributed patterns of explosive eruptive activity. *Bulletin of Volcanology*, *54*(1), 57–67. https://doi.org/10.1007/BF00278206

Deligne, N., Coles, S., & Sparks, R. (2010). Recurrence rates of large explosive volcanic eruptions. *Journal of Geophysical Research: Solid Earth*, *115*(B6), B06203. https://doi.org/10.1029/2009JB006554

Di Giacomo, D., Engdahl, E., & Storchak, D. (2018). The ISC-GEM earthquake catalogue (1904–2014): Status after the extension project. *Earth System Science Data*, *10*(4), 1877–1899. https://doi.org/10.5194/essd-10-1877-2018

Dziewonski, A., Chou, T.-A., & Woodhouse, J. (1981). Determination of earthquake source parameters from waveform data for studies of global and regional seismicity. *Journal of Geophysical Research: Solid Earth*, *86*(B4), 2825–2852. https://doi.org/10.1029/JB086iB04p02825

Ekström, G., Nettles, M., & Dziewoński, A. (2012). The global CMT project 2004–2010: Centroid-moment tensors for 13,017 earthquakes. *Physics of the Earth and Planetary Interiors*, *200*, 1–9. https://doi.org/10.1016/j.pepi.2012.04.002

Furlan, C. (2010). Extreme value methods for modelling historical series of large volcanic magnitudes. *Statistical Modelling*, *10*(2), 113–132. https://doi.org/10.1177/1471082x0801000201

Girona, T., Huber, C., & Caudron, C. (2018). Sensitivity to lunar cycles prior to the 2007 eruption of Ruapehu volcano. *Scientific Reports*, *8*(1), 1476. https://doi.org/10.1038/s41598-018-19307-z

Global Volcanism Program (2013). *Volcanoes of the world, v. 4.9.1*. Smithsonian Institution. https://doi.org/10.5479/si.GVP.VOTW4-2013

Gusev, A. (2008). Temporal structure of the global sequence of volcanic eruptions: Order clustering and intermittent discharge rate. *Physics of the Earth and Planetary Interiors*, *166*(3–4), 203–218. https://doi.org/10.1016/j.pepi.2008.01.004

Gusev, A. (2014). The fractal structure of the sequence of volcanic eruptions worldwide: Order clustering of events and episodic discharge of material. *Journal of Volcanology and Seismology*, *8*(1), 34–53. https://doi.org/10.1134/S0742046314010023

Hill, D. P., Pollitz, F., & Newhall, C. (2002). Earthquake-volcano interactions. *Physics Today*, *55*(11), 41–47. https://doi.org/10.1063/1.1535006

Huybers, P., & Langmuir, C. (2009). Feedback between deglaciation, volcanism, and atmospheric CO_2. *Earth and Planetary Science Letters*, *286*(3–4), 479–491. https://doi.org/10.1016/j.epsl.2009.07.014

International Seismological Centre (2020). *ISC-GEM earthquake catalogue*. https://doi.org/10.31905/d808b825

Johnson, C., Bürgmann, R., & Pollitz, F. (2015). Rare dynamic triggering of remote $M \geq 5.5$ earthquakes from global catalog analysis. *Journal of Geophysical Research: Solid Earth*, *120*(3), 1748–1761. https://doi.org/10.1002/2014JB011788

Jull, M., & McKenzie, D. (1996). The effect of deglaciation on mantle melting beneath Iceland. *Journal of Geophysical Research: Solid Earth*, *101*(B10), 21815–21828. https://doi.org/10.1029/96JB01308

Kutterolf, S., Jegen, M., Mitrovica, J. X., Kwasnitschka, T., Freundt, A., & Huybers, P. J. (2013). A detection of Milankovitch frequencies in global volcanic activity. *Geology*, *41*(2), 227–230. https://doi.org/10.1130/G33419.1

Larsen, G. (2000). Holocene eruptions within the Katla volcanic system, south Iceland: Characteristics and environmental impact. *Jökull Journal*, *49*, 1–28.

Lay, T. (2015). The surge of great earthquakes from 2004 to 2014. *Earth and Planetary Science Letters*, *409*, 133–146. https://doi.org/10.1016/j.epsl.2014.10.047

Levin, B., Sasorova, E., Gurianov, V., & Yarmolyuk, V. (2019). The relationship between global volcanic activity and variations in the velocity of Earth's rotation. In *Doklady Earth Sciences* (Vol. 484, pp. 146–150). https://doi.org/10.1134/S1028334X19020223

Linde, A. T., & Sacks, I. (1998). Triggering of volcanic eruptions. *Nature*, *395*, 888–890. https://doi.org/10.1038/27650

Luginbuhl, M., Rundle, J., & Turcotte, D. (2018). Natural time and nowcasting earthquakes: Are large global earthquakes clustered? *Pure and Applied Geophysics*, *175*, 661–670. https://doi.org/10.1007/s00024-018-1778-07

Marzocchi, W. (2002). Remote seismic influence on large explosive eruptions. *Journal of Geophysical Research: Solid Earth*, *107*(B1), EPM-6-1–EPM-6-7. https://doi.org/10.1029/2001JB000307

Mason, B., Pyle, D., Dade, W., & Jupp, T. (2004). Seasonality of volcanic eruptions. *Journal of Geophysical Research: Solid Earth*, *109*(B4), B04206. https://doi.org/10.1029/2002JB002293

Mead, S., & Magill, C. (2014). Determining change points in data completeness for the Holocene eruption record. *Bulletin of Volcanology*, *76*(11), 874. https://doi.org/10.1007/s00445-014-0874-y

Métivier, L., de Viron, O., Conrad, C., Renault, S., Diament, M., & Patau, G. (2009). Evidence of earthquake triggering by the solid earth tides. *Earth and Planetary Science Letters*, *278*(3–4), 370–375. https://doi.org/10.1016/j.epsl.2008.12.024

Michael, A. (2011). Random variability explains apparent global clustering of large earthquakes. *Geophysical Research Letters*, *38*(21), L21301. https://doi.org/10.1029/2011GL049443

Newhall, C., & Self, S. (1982). The volcanic explosivity index (VEI) an estimate of explosive magnitude for historical volcanism. *Journal of Geophysical Research: Oceans*, *87*(C2), 1231–1238. https://doi.org/10.1029/JC087iC02p01231

Nishimura, T. (2017). Triggering of volcanic eruptions by large earthquakes. *Geophysical Research Letters*, *44*(15), 7750–7756. https://doi.org/10.1002/2017GL074579

Olivieri, M., & Spada, G. (2015). Ice melting and earthquake suppression in Greenland. *Polar science*, *9*(1), 94–106. https://doi.org/10.1016/j.polar.2014.09.004

Pagli, C., & Sigmundsson, F. (2008). Will present day glacier retreat increase volcanic activity? Stress induced by recent glacier retreat and its effect on magmatism at the Vatnajökull ice cap, Iceland. *Geophysical Research Letters*, *35*(9), L09304. https://doi.org/10.1029/2008GL033510

Palladino, D., & Sottili, G. (2014). Earth's spin and volcanic eruptions: Evidence for mutual cause-and-effect interactions? *Terra Nova*, *26*(1), 78–84. https://doi.org/10.1111/ter.12073

Papale, P. (2018). Global time-size distribution of volcanic eruptions on Earth. *Scientific Reports*, *8*(1), 1–11. https://doi.org/10.1038/s41598-018-25286-y

Parsons, T., & Geist, E. (2012). Were global $M \geq 8.3$ earthquake time intervals random between 1900 and 2011? *Bulletin of the Seismological Society of America*, *102*(4), 1583–1592. https://doi.org/10.1785/0120110282

Parsons, T., Segou, M., & Marzocchi, W. (2014). The global aftershock zone. *Tectonophysics*, *618*, 1–34. https://doi.org/10.1016/j.tecto.2014.01.038

Parsons, T., & Velasco, A. (2011). Absence of remotely triggered large earthquakes beyond the mainshock region. *Nature Geoscience*, *4*(5), 312–316. https://doi.org/10.1038/ngeo1110

Pollitz, F., Stein, R., Sevilgen, V., & Bürgmann, R. (2012). The 11 April 2012 east Indian Ocean earthquake triggered large aftershocks worldwide. *Nature*, *490*(7419), 250–253. https://doi.org/10.1038/nature11504

Rampino, M., Self, S., & Fairbridge, R. (1979). Can rapid climatic change cause volcanic eruptions? *Science*, *206*(4420), 826–829. https://doi.org/10.1126/science.206.4420.826

Rawson, H., Pyle, D., Mather, T., Smith, V., Fontijn, K., Lachowycz, S., & Naranjo, J. (2016). The magmatic and eruptive response of arc volcanoes to deglaciation: Insights from southern Chile. *Geology*, *44*(4), 251–254. https://doi.org/10.1130/G37504.1

Rogerson, P. (2018). Statistical evidence for long-range space-time relationships between large earthquakes. *Journal of Seismology*, *22*(6), 1423–1435. https://doi.org/10.1007/s10950-018-9775-4

Romanowicz, B. (1993). Spatiotemporal patterns in the energy release of great earthquakes. *Science*, *260*(5116), 1923–1926. https://doi.org/10.1126/science.260.5116.1923

Rougier, J., Sparks, R., & Cashman, K. (2016). Global recording rates for large eruptions. *Journal of Applied Volcanology*, *5*(1), 11. https://doi.org/10.1186/s13617-016-0051-4

Rougier, J., Sparks, R., & Cashman, K. (2018). Regional and global under-recording of large explosive eruptions in the last 1000 years. *Journal of Applied Volcanology*, *7*(1), 1–10. https://doi.org/10.1186/s13617-017-0070-9

Rougier, J., Sparks, R., Cashman, K., & Brown, S. (2018). The global magnitude-frequency relationship for large explosive volcanic eruptions. *Earth and Planetary Science Letters*, *482*, 621–629. https://doi.org/10.1016/j.epsl.2017.11.015

Sawi, T. M., & Manga, M. (2018). Revisiting short-term earthquake triggered volcanism. *Bulletin of Volcanology*, *80*(7), 57. https://doi.org/10.1007/s00445-018-1232-2

Scholz, C., Tan, Y., & Albino, F. (2019). The mechanism of tidal triggering of earthquakes at mid-ocean ridges. *Nature Communications*, *10*, 2526. https://doi.org/10.1038/s41467-019-10605-2

Seropian, G., Kennedy, B., Walter, T., Ichihara, M., & Jolly, A. (2021). A review framework of how earthquakes trigger volcanic eruptions. *Nature Communications*, *12*(1), 1–13. https://doi.org/10.1038/s41467-021-21166-8

Shanker, D., Kapur, N., & Singh, V. (2001). On the spatio temporal distribution of global seismicity and rotation of the Earth—A review. *Acta Geodaetica et Geophysica Hungarica*, *36*(2), 175–187. https://doi.org/10.1556/AGeod.36.2001.2.5

Shearer, P., & Stark, P. (2012). Global risk of big earthquakes has not recently increased. *Proceedings of the National Academy of Sciences*, *109*(3), 717–721. https://doi.org/10.1073/pnas.1118525109

Storchak, D., Di Giacomo, D., Bondár, I., Engdahl, E., Harris, J., Lee, W., et al. (2013). Public release of the ISC-GEM global instrumental earthquake catalogue (1900–2009). *Seismological Research Letters*, *84*(5), 810–815. https://doi.org/10.1785/0220130034

Storchak, D., Di Giacomo, D., Engdahl, E., Harris, J., Bondár, I., Lee, W., et al. (2015). The ISC-GEM global instrumental earthquake catalogue (1900–2009): Introduction. *Physics of the Earth and Planetary Interiors*, *239*, 48–63. https://doi.org/10.1016/j.pepi.2014.06.009

Tuel, A., Naveau, P., & Ammann, C. (2017). Skillful prediction of multidecadal variations in volcanic forcing. *Geophysical Research Letters*, *44*(6), 2868–2874. https://doi.org/10.1002/2016GL072234

Wyss, M., & Toya, Y. (2000). Is background seismicity produced at a stationary Poissonian rate? *Bulletin of the Seismological Society of America*, *90*(5), 1174–1187. https://doi.org/10.1785/0119990158

Zaliapin, I., & Kreemer, C. (2017). Systematic fluctuations in the global seismic moment release. *Geophysical Research Letters*, *44*(10), 4820–4828. https://doi.org/10.1002/2017GL073504